Third-harmonic generation in silicon photonic crystals and microcavities

M. G. Martemyanov, E. M. Kim, T. V. Dolgova, A. A. Fedyanin, and O. A. Aktsipetrov*
Department of Physics, Moscow State University, 119992 Moscow, Russia

G. Marowsky
Laser-Laboratorium Göttingen, D-37077 Göttingen, Germany
(Received 25 September 2003; revised manuscript received 14 June 2004; published 30 August 2004)

Third-harmonic generation (THG) is observed in photonic crystals and microcavities formed from porous silicon. The THG spectra reveal an intensity enhancement at the photonic band gap edge of these photonic crystals and at the resonance of the fundamental radiation with the microcavity mode. The enhancement is related to the combination of the phase matching and fundamental light localization. The amplitudes of the THG peaks are strongly affected by the competition between the porous silicon absorption at the third-harmonic wavelength and the three-photon resonance of cubic susceptibility of silicon achieved in the vicinity of the E_0'/E_1 critical point.

DOI: 10.1103/PhysRevB.70.073311 PACS number(s): 78.67.−n, 42.65.Ky, 42.70.Qs

Nonlinear-optical phenomena in photonic band gap (PBG) materials are determined by electron energy spectrum of the host materials, electromagnetic modes configuration and effective dispersion relations in PBG structures.[1–3] Resonances in electron energy spectrum of forming materials, which are singularities in electron band structure, yield the resonances in nonlinear susceptibilities. Together with peculiarities in the group velocity behavior and density of optical modes inside photonic crystals, this strongly controls the nonlinear response of photonic crystals on the optical field. For example, large cubic nonlinearity, along with the balance between the anomalous group velocity dispersion and the self-phase modulation, allows the gap solitons formation in photonic crystals.[4] The fulfillment of phase-matching conditions in photonic crystals with large quadratic susceptibility leads to a significant enhancement of second-harmonic generation (SHG), if the second-harmonic (SH) or fundamental wavelength coincides with the PBG edge.[5] The local enhancement of the electromagnetic field or the intensity-dependent refractive index lead, for instance, to optical bistability observed in photonic crystals with a large cubic nonlinearity.[6] The optical wave localization at the defect of a photonic crystal or at the spacer of a photonic-crystal microcavity (MC) enhances manyfold the SHG response, which has been recently observed in MCs with chromophore,[7] polymeric,[8] or semiconductor[9,10] spacers.

The problem of a third-harmonic generation (THG) enhancement in photonic crystals has been intensively discussed during the last several years. Theoretical studies predict an intensity enhancement at the PBG edge by means of the direct coupling of three fundamental photons via the cubic susceptibility $\chi^{(3)}$ (Ref. [11]) or due to cascade processes of second-harmonic and sum-frequency generation, $\omega+2\omega$, via the quadratic susceptibility $\chi^{(2)}$.[12] The small group velocity of the fundamental radiation implements the phase mismatch compensation at the PBG edge.[13] The local enhancement of a transient standing wave in finite-size photonic crystals[14] is also expected to contribute to the THG efficiency by analogy with efficient SHG observed recently in photonic crystals fabricated from stratified semiconductors.[15]

In this paper, enhanced THG is observed in one-dimensional photonic crystals and microcavities. The THG spectra measured both in frequency and wave-vector domains reveal the intensity enhancement, when the fundamental radiation is tuned across the PBG edge as well as in resonance with the MC mode. The peak at the band edge is common for photonic crystals, while the THG resonance at the mode originates from the microcavity and strongly depends on the MC quality factor.

Photonic-crystal microcavities are grown from mesoporous silicon. The high quality factor ($Q \simeq 10^2$) and the high reflectance ($T \simeq 0.95$) in the PBG are achieved by the large contrast in porosities and, therefore, in the refractive indices of adjacent layers, achieving values up to $\Delta n \simeq 0.7$.[16] Controllable variation of the pore size allows the PBG tuning. Significant enhancement of photoluminescence and Raman scattering, observed in photonic crystals and MCs formed from porous silicon,[16] also proves their high quality factor. Recently, fascinating band-edge effects in optical pulse propagation have been observed in Fibonacci quasicrystals fabricated from several hundred layers of mesoporous silicon.[17]

Microcavities are fabricated by the conventional electrochemical etching procedure[16] using p^+-type Si(001) wafers with resistivity of 0.005 Ω cm. The modulation of the refractive index along the surface normal z is achieved by the time variation of the etching current. The thickness of the mesoporous silicon layers is controlled by the etching time. The optical thicknesses of the layers are calibrated using the reflectance spectra of the single porous silicon layers. Atomic-force microscopy images show that the typical pore size is in order of 30 nm and significantly smaller than the optical wavelength. MCs are designed to possess the PBG for oblique angles of incidence below 900 nm, where optical absorption is negligible, and with the MC mode in the vicinity of the three-photon $\chi^{(3)}$ resonance corresponding to the E_0'/E_1 critical point of the silicon band structure.[18] The latter is chosen to compensate the significant UV absorption of porous silicon.[19] The samples consist of a half-wavelength-

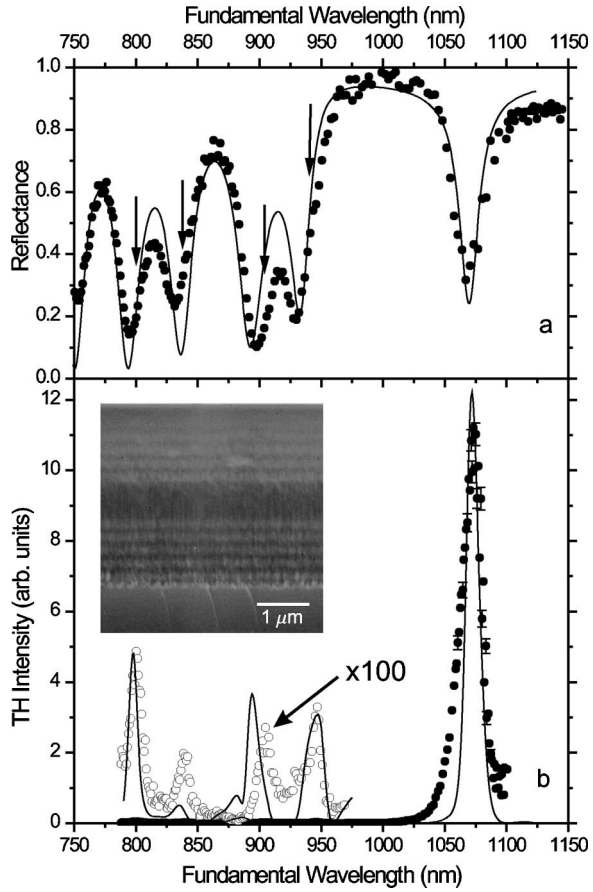

FIG. 1. (a) The reflectance spectrum of the *s*-polarized light from porous silicon microcavity. Arrows indicate positions of the peaks in the THG spectrum. (b) Closed circles: the THG spectrum measured in the *s*-in, *s*-out polarization combination. Open circles: the 100 times magnified part of the spectrum. Lines are the fit to data using nonlinear-transfer matrix formalism. The inset shows scanning electron microscope image of porous silicon microcavity.

thick cavity spacer ($\lambda_{MC} \simeq 1300$ nm) sandwiched between two distributed Bragg reflectors formed from five pairs of quarter-wavelength-thick layers (inset in Fig. 1). λ_{MC} denotes the MC mode for normal incidence. The refractive indices of the layers in the Bragg reflectors are $n_H \simeq 1.9$ and $n_L \simeq 1.6$, the thicknesses are $d_H \simeq 170$ nm and $d_L \simeq 200$ nm, and the porosities are $f_H \simeq 0.64$ and $f_L \simeq 0.77$, respectively. The cavity spacer thickness is $d_{MC} = 2d_L$. The *Q*-factor is slightly below 10^2 and restricted by losses due to light scattering in the pores. A high UV absorption of the silicon substrate imposes the reflection experimental geometry.

The tuning of the fundamental radiation across the PBG edge and the resonance of the fundamental wave with the MC mode, $k_z d_{MC} = \pi$, where k_z is the normal component of the fundamental wave vector inside the MC spacer, is achieved in both frequency and wave-vector domains. THG spectroscopy in the frequency domain is realized by tuning the fundamental wavelength, λ_ω, at fixed angle of incidence, θ. In wave-vector domain THG spectroscopy, θ is varied at fixed λ_ω. The 4-ns-pulsed output of the optical parametric oscillator tunable from 750 to 1300 nm and the 10-ns-pulsed infrared output of the Nd^{3+}:YAG laser with

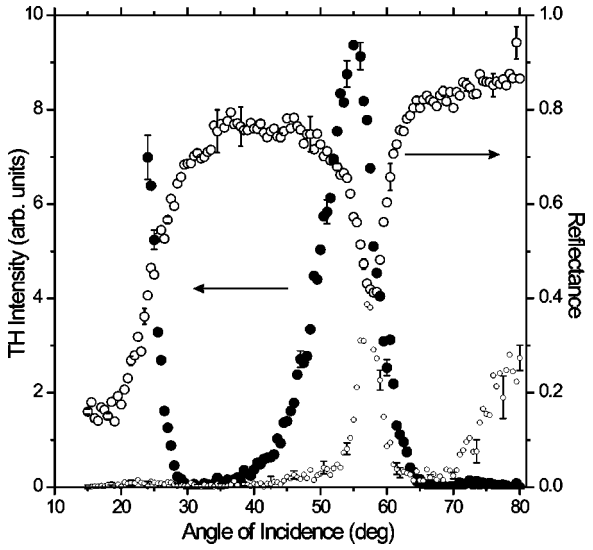

FIG. 2. Closed circles: the angular THG spectrum of the porous silicon MC measured in the *p*-in, *p*-out polarization combination. Open circles: the reflectance spectrum of the *s*-polarized radiation of 1064 nm. Small circles: the angular spectrum of the SH intensity measured in the *s*-in, *p*-out polarization combination.

energy below 5 mJ/pulse are used. The third-harmonic (TH) radiation is separated by a set of appropriate color filters and detected by a photomultiplier tube. A monochromator is used to check the spectral background.

Figure 1 shows reflection and THG spectra measured in the frequency domain at $\theta = 45°$. The PBG is located at $\lambda_\omega > 950$ nm, where reflectance is close to unity. The MC mode is centered at $\lambda_\omega \simeq 1072$ nm. The THG spectrum has a peak, which coincides with the MC mode. The TH intensity is approximately 5×10^3 times larger in comparison with that in the pass band. The other THG peaks, magnified in Fig. 1(b), are approximately 500 times smaller. They correlate with the minima in the reflectance spectrum being slightly redshifted. The largest shift of 15 nm is observed at the short-wavelength PBG edge. THG is strongly suppressed out of these peaks in both the photonic band gap and the pass band. Figure 2 shows the THG spectrum measured in the wave-vector domain. The TH intensity reveals an enhancement at $\theta \simeq 55°$, which is close to the MC mode, and resonance in SHG located at $\theta \simeq 58°$. The THG peak is approximately two times broader than the MC mode drop of the linear reflection. This is apparently associated with smaller *Q*-factor value for the *p*-polarized fundamental radiation than that for the *s*-polarized one. The shift of the THG peak from the mode position and the SHG peak stems from different mode positions of the *s*- and *p*-polarized fundamental light. The TH intensity increases also at the short-wavelength PBG edge for $\theta < 30°$. This THG growth is even stronger than the enhancement at the MC mode.

The electric-dipole cubic polarization, $\mathbf{P}^{(3)}(3\omega) = \chi^{(3)} \vdots \mathbf{E}(\omega)\mathbf{E}(\omega)\mathbf{E}(\omega)$, is supposed to be the only source of THG in porous silicon MCs. Cascade THG is neglected since small electric-dipole SHG is expected only at the pore surfaces due to the inversion symmetry of the bulk silicon. Each porous silicon layer is considered as macroscopically in-

plane isotropic film having nine nonzero $\chi^{(3)}$ elements: $\chi^{(3)}_{yyzz}=\chi^{(3)}_{xxzz}$, $\chi^{(3)}_{zzzz}$, $\chi^{(3)}_{zzxx}=\chi^{(3)}_{zzyy}$ and $\chi^{(3)}_{iijj}=1/3\chi^{(3)}_{iiii}$ with $i,j=x,y$. The symmetry considered is confirmed by the THG enhancement for the *p*-in, *p*-out and *s*-in, *s*-out polarization combinations and negligible TH intensity in the *p*-in, *s*-out and *s*-in, *p*-out polarization combinations.

The primary mechanism of the THG enhancement at the MC mode is the fundamental light localization inside the MC spacer and the surrounding layers of the Bragg reflectors. The spatial distribution of the resonant fundamental radiation across the MC with similar parameters was probed at the MC cleavage by scanning near-field optical microscopy.[10] These direct studies revealed the six- to eight fold enhancement of the amplitude of the standing wave inside the MC spacer with respect to the incoming field in agreement with calculations performed using the matrix formalism. The partial contributions of the MC spacer and the surrounding layers of the Bragg reflectors to the total TH field are obtained using nonlinear transfer-matrix technique.[20] It is shown that the phase shift between dominating THG contributions does not exceed $\pi/2$ providing their constructive interference.[21] In some sense, such interference is equivalent to the phase matching since the optical path inside the MC spacer is effectively Q times extended at the MC mode.

The combined fit to reflectance and THG spectra using nonlinear transfer matrices is shown in Fig. 1 and demonstrates a good agreement with experimental data. The THG peaks at the PBG edge and at the minima of the reflectance spectrum are treated as THG resonances in photonic crystals due to the small role of the MC spacer in the formation of the PBG edge. The fundamental field with the wavelength at the PBG edge penetrates efficiently to photonic crystals. The THG enhancement stems from constructive interference of the partial THG contributions of the layers, which accomplishes effective phase matching.[21] Additional enhancement of the partial TH field amplitudes is provided due to the fundamental field localization in the finite-size photonic crystals.[14] Absorption in porous silicon at the TH wavelength varies both the amplitude and the phase of the partial TH fields lessening the amplitudes of the THG peaks. To reduce the phase mismatch the specially designed MC is grown, in which the optical thickness of the jth layer of the Bragg reflector is steadily decreased with the layer number, $n_j d_j = \lambda_{MC}/4 - j\eta$. The reflectivity spectrum of MC fabricated with $\eta=0.8$ nm is shown in Fig. 3. Apart from the drop at the MC mode, the spectrum has a feature at the PBG edge at $\lambda_\omega \simeq 942$ nm. The THG spectrum has the peak at $\lambda_\omega \simeq 1074$ nm, which correlates with the MC mode, and two other peaks at $\lambda_\omega \simeq 952$ nm and $\lambda_\omega \simeq 1173$ nm. They correspond to PBG edges and have the amplitudes comparable with the THG peak at the MC mode. The intensity enhancement is observed also at $\lambda_\omega \simeq 838$ nm, which almost coincides with the minimum in the reflectance spectrum. However, the THG efficiency both at the band edge and the mode is restricted by the significant porous silicon absorption at the TH wavelength[19] estimated to be approximately 10^4 cm^{-1} at 370 nm for porosity of $f \simeq 0.77$. Absorption losses are compensated by the resonance of the cubic susceptibility of porous silicon at the TH wavelength. The spectrum $\chi^{(3)}(3\omega)$ is supposed to be similar to that of the crystalline silicon with

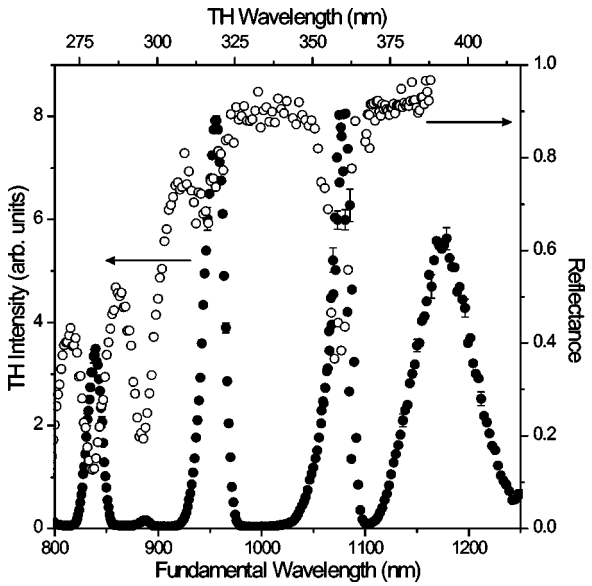

FIG. 3. Closed circles: THG spectrum of MC with monotonously modified layer thickness measured for $\theta=45°$ in the *s*-in, *s*-out polarization combination. Open circles: reflectance spectrum of the *s*-polarized fundamental radiation.

the three-photon resonance at $\lambda_\omega \simeq 1100$ nm corresponding to the E_0'/E_1 critical point of the silicon band structure.[18] In silicon, the resonance contributions from critical points of combined density of electron states dominates the nonlinear susceptibilities spectra. In spite of absorption losses, the

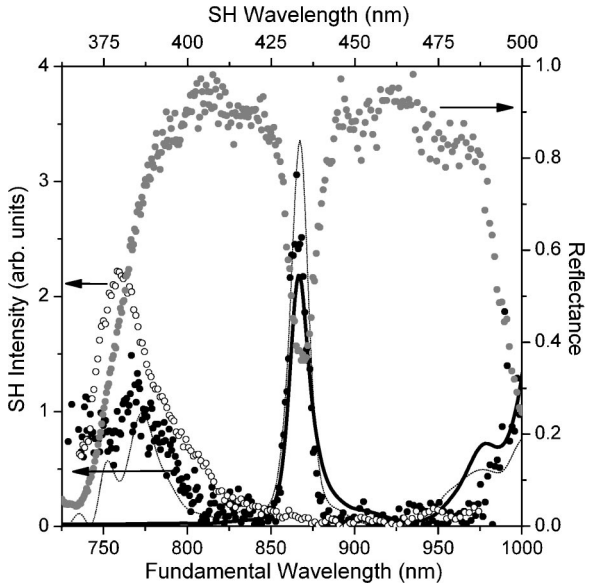

FIG. 4. Closed circles: SHG spectrum of MC for $\theta=30°$. The peak at the MC mode and the SHG growth at the long-wavelength-edge of PBG due to the resonance of the fundamental radiation with the MC mode and the phase-matching at the PBG edge (Ref. 10) are seen. Open circles: SHG spectrum of the Si(001) surface. Gray circles: reflection spectrum of the *s*-polarized fundamental radiation. Curves: the SHG spectra of MC calculated using nonlinear transfer matrix technique with Lorenz line shape of $\chi^{(2)}$ (dashed curve) and with the spectral-independent $\chi^{(2)}$ (solid curve).

THG efficiency at the $\chi^{(3)}$ resonance is significantly larger in comparison with that in the transparency band. Thus, the combination of large density of optical modes at the fundamental wavelength and the singularity of electron density of states providing the $\chi^{(3)}$ resonance at the TH wavelength yields the optimal conditions for the enhancement of the TH intensity in silicon photonic crystals.

The basic role of electron resonances of nonlinear susceptibilities in the enhancement of the nonlinear-optical response is evident for giant SHG in silicon PBG structures. Figure 4 shows the SH intensity spectrum of MC with $\lambda_{MC} \simeq 945$ nm measured in the *s*-in, *p*-out polarization combination. The significant enhancement of the SH intensity is observed at the short-wavelength edge of PBG, where phase matching is expected only for the anomalous dispersion. The SHG spectrum of the Si(001) substrate measured in the *p*-in, *p*-out polarization combination has a peak at the similar spectral position corresponding to the two-photon resonance at the E_0'/E_1 silicon critical point. Thus the SHG enhancement at the short-wavelength PBG edge is attributed entirely to the electron $\chi^{(2)}$ resonances.

In conclusion, THG spectroscopy of one-dimensional photonic crystals formed from mesoporous silicon reveals an intensity enhancement at the PBG edge up to 10^3 in comparison with that outside the photonic band gap. The THG enhancement is interpreted as the result of effective phase-mismatch compensation and the fundamental field localization in the finite-size Bragg reflectors. The 5×10^3 enhancement of the TH intensity is observed if the fundamental radiation is in resonance with the mode of photonic-crystal microcavities. This THG peak originates from the fundamental field localization inside the MC spacer. The resonance features of electron energy spectrum of the host silicon in the vicinity of the E_0'/E_1 critical point reveals the interplay of silicon absorption and the $\chi^{(3)}$ resonance at the TH wavelength. These results indicate that photonic crystal and microcavity effects offer a practical means of controlling the THG enhancement. The use of electrochemical microstructuring to control the nonlinear-optical response of silicon presents future opportunities for optical applications utilizing all-silicon technology.

This work is supported in part by the Russian Foundation for Basic Research (Grants No. 04-02-16847, 03-02-39010 and 01-02-04018), the Presidential Grant for Leading Russian Science Schools (No. 1604.2003.2), DFG Grant No. 436 RUS 113/640/0-1, NATO Grant PST.CLG.979406, and the INTAS Grant No. 03-51-3784.

*URL: http://www.shg.ru

[1] E. Yablonovitch, Phys. Rev. Lett. **58**, 2059 (1987); S. John, *ibid.* **58**, 2486 (1987).

[2] M. Scalora, J.P. Dowling, C.M. Bowden, and M.J. Bloemer, Phys. Rev. Lett. **73**, 1368 (1994).

[3] O.A. Aktsipetrov, A.A. Fedyanin, E.D. Mishina, A.A. Nikulin, A.N. Rubtsov, C.W. van Hasselt, M.A.C. Devillers, and Th. Rasing, Phys. Rev. Lett. **78**, 46 (1997).

[4] W. Chen and D.L. Mills, Phys. Rev. Lett. **58**, 160 (1987); B.J. Eggleton, R.E. Slusher, C.M. de Sterke, P.A. Krug, and J.E. Sipe, *ibid.* **76**, 1627 (1996).

[5] A.V. Balakin, V.A. Bushuev, N.I. Koroteev, B.I. Mantsyzov, I.A. Ozheredov, A.P. Shkurinov, D. Boucher, and P. Masselin, Opt. Lett. **24**, 793 (1999); Y. Dumeige, P. Vidakovic, S. Sauvage, I. Sagnes, J.A. Levenson, C. Sibilia, M. Centini, G. D'Aguanno, and M. Scalora, Appl. Phys. Lett. **78**, 3021 (2001).

[6] C.J. Herbert and M.S. Malcuit, Opt. Lett. **18**, 1783 (1993); A.R. Cowan and J.F. Young, Phys. Rev. E **68**, 046606 (2003).

[7] J. Trull, R. Vilaseca, J. Martorell, and R. Corbalan, Opt. Lett. **20**, 1746 (1995).

[8] H. Cao, D.B. Hall, J.M. Torkelson, and C.-Q. Cao, Appl. Phys. Lett. **76**, 538 (2001).

[9] S. Lettieri, S. Di Finizio, P. Maddalena, V. Ballarini, and F. Giorgis, Appl. Phys. Lett. **81**, 4706 (2002).

[10] T.V. Dolgova, A.I. Maidykovski, M.G. Martemyanov, A.A. Fedyanin, O.A. Aktsipetrov, G. Marowsky, V.A. Yakovlev, and G. Mattei, Appl. Phys. Lett. **81**, 2725 (2002).

[11] V.V. Konotop and V. Kuzmiak, J. Opt. Soc. Am. B **16**, 1370 (1999).

[12] M. Centini, G. D'Aguanno, M. Scalora, C. Sibilia, M. Bertolotti, M.J. Bloemer, and C.M. Bowden, Phys. Rev. E **64**, 046606 (2001).

[13] M. Scalora, M.J. Bloemer, A.S. Manka, J.P. Dowling, C.M. Bowden, R. Viswanathan, and J.W. Haus, Phys. Rev. A **56**, 3166 (1997).

[14] M. Centini, C. Sibilia, M. Scalora, G. D'Aguanno, M. Bertolotti, M.J. Bloemer, C.M. Bowden, and I. Nefedov, Phys. Rev. E **60**, 4891 (1999).

[15] Y. Dumeige, I. Sagnes, P. Monnier, P. Vidakovic, I. Abram, C. Meriadec, and A. Levenson, Phys. Rev. Lett. **89**, 043901 (2002).

[16] O. Bisi, S. Ossicini, and L. Pavesi, Surf. Sci. Rep. **38**, 1 (2000).

[17] L. Dal Negro, C.J. Oton, Z. Gaburro, L. Pavesi, P. Johnson, Ad Lagendijk, R. Righini, M. Colocci, and D.S. Wiersma, Phys. Rev. Lett. **90**, 055501 (2003).

[18] P. Lautenschlager, M. Garriga, L. Vina, and M. Cardona, Phys. Rev. B **36**, 4821 (1987).

[19] A. Kux and M. Ben Chorin, Phys. Rev. B **51**, 17 535 (1995); D. Kovalev, G. Polisski, M. Ben Chorin, J. Diener, and F. Koch, J. Appl. Phys. **80**, 5978 (1996).

[20] D.S. Bethune, J. Opt. Soc. Am. B **6**, 910 (1989).

[21] M.G. Martemyanov, T.V. Dolgova, and A.A. Fedyanin, JETP **98**, 463 (2004).